time points and then dividing the point-by-point changes by the standard deviation of the paired-measurement noise. The standardized thickness points with z-values lower than 1.96 (p < 0.05) were marked and counted as points with significant cartilage loss. The proportion of marked points was reported as the percentage of significant cartilage loss at the femur cartilage and the tibia cartilage. Finally, all the 12-month and 24-month change maps were aggregated into a single standardized change map. The significant cartilage loss maps were aggregated into a single heat-map that showed the prevalence and localization of the significant changes in cartilage thickness. The difference between 24-month changes and 12-month changes were used to estimate the standardized response of the mean (SRM) of the methodology.

Results: One knee observation was dropped due to poor segmentation quality. As seen in Fig. 1, heat maps showed different patterns of loss among the no-denuded, the low-denuded and the high-denuded groups. The entire femur showed an average significant 12-month loss on 6.9% of its surface. The loss progressed towards an 8.9% loss with a SRM of 0.48 (0.31 to 0.65). The tibia progressed from a 7.0% loss to an 8.6% loss with a SRM of 0.25 (0.08 to 0.42). The knees with no-denuded areas showed cartilage loss at 5.4% of their femoral cartilage and progressed towards a 7.8% loss with a SRM of 0.73 (0.45 to 1.01) and 74.5% (60.1% to 85.2%) of the knees worsening the affected area. The tibia progressed from a 5.9% loss towards a 7.9% loss with a SRM of 0.39 (0.11 to 0.67). Subjects with small denuded areas showed a 12-month, 24-month loss of 7.1%, 8.6% respectively with a 0.36 SRM in the entire femur. Subjects with large denuded areas showed a 12-month, 24-month loss of 9.1%, 11.0% respectively with a 0.36 SRM.

Conclusion: The image analysis technology used in this study provided quantitative and statistical maps that showed the prevalence and location of changes in cartilage thickness. The spatial localization and the prevalence of those changes were different in the different OA groups studied in this work, indicating the degree of heterogeneity of the disease presentation and progression. Furthermore, the methodology showed that early stage OA (Bone free of denuded areas) is very dynamic with cartilage loss progressing at the annual rate of 2.2% (0.45 < SRM < 1.01). Future work will compare the rate and localization of the changes among the non-exposed OAI cohort, a symptomatic worsening OAI group, and an age matched symptom stable OAI group.
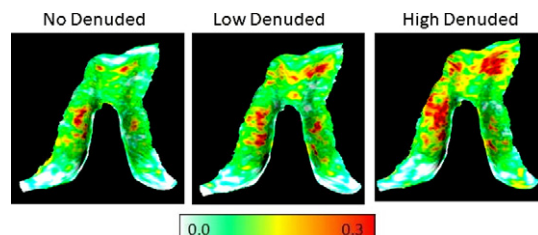

Fig. 1. Heat map of proportion of subjects that show significant changes in cartilage thickness in three different populations.

394

PREDICTION OF THE ONSET OF KNEE PAIN BY QUANTITATIVE MRI: DATA FROM THE OSTEOARTHRITIS INITIATIVE

J.G. Tamez-Pena[1,2], P. Gonzalez[2], E. Schreyer[2], S. Tottermann[2]. [1]Tec de Monterrey, Monterrey, Nuevo Leon, Mexico; [2]Qmetrics Technologies, Rochester, NY, USA

Purpose: The purpose of this study was to evaluate the ability of structural changes in cartilage thickness to predict the future onset of knee pain as measured by the KOOS pain.

Methods: The symptomatic knee of 138 subjects at baseline, 12 month and 24 month DESS sagittal MRI knee images from OAI data progression cohort releases 0.C.2, 1.C.2 and 3.C.1 were segmented by a multi-atlas based segmentation algorithm. Images were evaluated for image quality and segmentation quality. All the local thicknesses measurements at the cartilage surface were projected back into the cartilage volume and mapped into to the digital atlas space. After that, cartilage voxels were compared voxel by voxel to the atlas' cartilage surface thicknesses creating atlas-referenced thickness maps. At baseline atlas-referenced maps of thickness values were statistically described by mean, variance and distribution percentiles. Furthermore, the 12 month data and the 24 month thickness maps were compared back to the baseline maps and

the voxel-by-voxel longitudinal thickness change maps for every subject were computed. The change maps were described by mean change, variance of change and proportions of areas with significant changes. The quantification of curvature and thickness were done on the central regions of the knee, the entire femur and tibia cartilage. The KOOS scores were downloaded from the OAI site (http://www.oai.ucsf.edu) and used to associate the quantitative MRI measurements to changes in KOOS pain. Only subjects with an enrolment KOOS pain larger than 80 were considered for this analysis. Individual subject changes between the 36 month, 24 month and 12 month to the enrolment assessment of KOOS pain were compared to each subject qMRI baseline assessment and to each subject proportion of significant thickness changes observed between the baseline observations to the 12month. Furthermore, the area under the curve (AUC) of the ROC was computed for the test of predicting a positive change in pain. Finally a linear model with enrolment BMI was constructed to further study the association of the qMRI data to the change in knee pain. Significant associations were defined by beta coefficients different from zero.

Results: One subject was removed due to poor segmentation quality. 43 subjects had a KOOS pain score greater than 80. Table 1 shows the association statistics. The atlas referenced standard deviation of cartilage thickness was a good predictor of an increase of pain at 12 month, 24 month and 36 month (Spearman r = 0.4, 0.42 and 0.31 respectively). Baseline to 12 month significant changes in tibia cartilage thickness were also associated to an increase in pain at 12, 24 and 36 month (Spearman r = 0.42, 0.34 and 0.34 respectively). The significant AUC were also found for the prediction of a 24 month increase of pain (AUC = 0.81) by the thickness referenced standard deviation. The linear model observed positive association of the atlas referenced standard deviation to the 24 month pain, and of the significant changes in tibia to the increase in 12 month pain. Figure 1 shows the ROC of the prediction of a 24 month vs. Baseline increase in pain. ROC curves indicate that an 80% prediction of pain onset can be achieved with less than 30% of false positives.

Association to Changes in KOOS Pain (n=43)

|		Baseline Measurements			Proportion of Significant Thickness Changes (V1-V0)		linear Model
		BMI	Femur		Femur	Tibia	
			Curvature	Thickness Std			
Spearman (r)	12 Month vs. BL	0.08(0.624)	0.19(0.223)	-0.40(0.008)*	-0.25(0.106)	-0.42(0.005)**	0.54(0.000)
	24 Month vs. BL	0.06(0.719)	0.24(0.123)	-0.42(0.005)**	-0.23(0.146)	-0.34(0.024)	0.43(0.004)
	36 Month vs. BL	0.17(0.271)	0.30(0.053)	-0.31(0.045)	-0.27(0.078)	-0.34(0.024)*	0.52(0.000)
ROC AUC	12 Month vs. BL	0.510	0.622	0.676	0.620	0.753	0.758
	24 Month vs. BL	0.546	0.663	0.819	0.751	0.756	0.826
	36 Month vs. BL	0.504	0.737	0.689	0.612	0.692	0.748
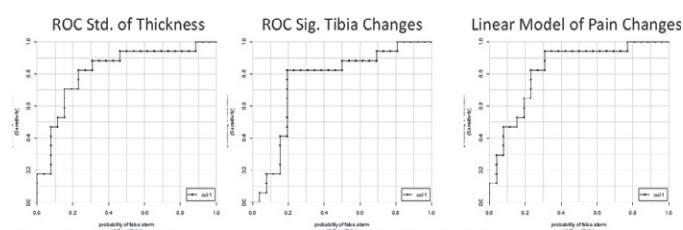
Fig. 1. Month vs Enrolment pain increase prediction ROC. Left: ROC curve of the atlas reference thickness. Middle: ROC curve of the significant changes in tibia thickness. Right: ROC of the linear model that includes BMI, curvature, standard deviation and significant changes.

Conclusion: The changes in cartilage morphology are good predictors of pain onset. ROC and correlation analysis indicate that structural changes in cartilage morphology can be used to predict the 2 year onset of knee pain with a true positive rate of 80% and 30% of false positives. These findings in combination with other risk factors can help in the design of prospective clinical trials requiring a good proportion of subjects showing significant progression in their pain symptoms.

395

OSTEOPHYTES AND JOINT SPACE NARROWING ARE INDEPENDENTLY ASSOCIATED WITH PAIN IN FINGER JOINTS IN HAND OSTEOARTHRITIS

M. Kortekaas, W-Y. Kwok, M. Reijnierse, T. Huizinga, M. Kloppenburg. *Leiden Univ. Med. Ctr., Leiden, Netherlands*

Purpose: Hand osteoarthritis (HOA) can cause considerable pain, and one could assume that structural abnormalities play a role in the aetiology of this clinical feature. However, in earlier studies only limited associations

were demonstrated. Explanations for the limited associations can be the usage of global and summated scores for pain and structural abnormalities, and not taking into account patients effects in earlier studies.

The objective of the present study was to investigate the association between structural abnormalities and pain. To prevent the above mentioned potential limitations associations were analysed at patient level and at individual joint level using both US and CR taking in account patient effects.

Methods: In consecutive patients, fullfilling the ACR criteria for HOA and at least 45 years of age, hand pain was assessed by VAS and AUSCAN pain. During physical examination 1st CMCJs, 1st IPJs, MCPJs, PIPJs and DIPJs from both hands were examined for pain upon palpation.With US all hand joints were scored for osteophytes, PDS, effusion and synovial thickening (0–3). Radiographs of both hands were scored for osteophytes (0–3) and JSN (0–3), following the OARSI atlas.

With linear regression analysis, summated scores of osteophytes or JSN were associated with clinical features adjusting for age, sex, body mass index (BMI) and inflammatory US features.

Generalized estimated equations (GEE) were used to study the relationship of structural abnormalities with pain on joint level, thus taking into account patient effects. Relative risks were presented as odds ratios (OR) with 95% confidence intervals (95%CI). Adjustments were made for confounders.

Results: Of 55 patients (mean age 61 years, 86% female) 1649 joints were studied: 69% had osteophytes on US and 46% on CR. JSN occurred in 47%. Structural abnormalities summated scores assessed on US or CR showed no association with AUSCAN pain, VAS pain or DI of the hands.

On joint level, both osteophytes showed strong dose-dependent associations with pain after adjustment for age, sex and BMI: osteophytes (grade 3): OR (95%CI): 6.2 (4.0–9.4)(US) and 4.8 (2.7–8.4)(CR). After adjustments for inflammatory US features and JSN the OR for US was 4.8 (3.1–7.5) and for CR of 4.1 (2.4–7.1)

JSN as well demonstrated strong dose-dependent associations with pain per joint: OR JSN (grade 3): 6.4 (2.7–14.8). After further adjustments for inflammatory US features and osteophytes: OR 4.2 (2.0–4.0). This means that both osteophytes and JSN are independently related to pain in HOA

Conclusions: Strong, dose-dependent associations were found between structural OA abnormalities and pain in separate hand joints studied by both US and CR. However, analyses must be performed on joint level taking into account patient's effects, or associations can be missed. Associations were found independently not only for osteophytes, but also for JSN, which is a new finding in HOA. In summary, these findings are important for our understanding of HOA and for elucidating the aetiology of pain.

396

COMPARISON OF NORMAL ARTICULAR CARTILAGE IMAGES ASSESSED BY HIGH FREQUENCY ULTRASOUND MICROSCOPE AND SCANNING ACOUSTIC MICROSCOPE

Y. Hagiwara[1], Y. Saijo[2], A. Ando[1], Y. Onoda[1], H. Suda[1], E. Chimoto[1], K. Hatori[3], E. Itoi[1]. *[1]Tohoku Univ. Graduate Sch. of Med., Dept. of Orthopaedic Surgery, Sendai, Japan; [2]Tohoku Univ. Graduate Sch. of BioMed. Engineering, Dept. of BioMed. Imaging, Sendai, Japan; [3]Tohoku Univ. Graduate Sch. of Dentistry, Div. of Advanced Prosthetic Dentistry, Sendai, Japan*

Purpose: Ultrasonography is a non-invasive and inexpensive method widely accepted in daily clinical use. However, the resolution of ordinary equipment for evaluating the articular cartilage is not sufficient to supersede a histological examination. The purpose of this study was to compare images of a newly developed high frequency ultrasound imaging system (HFUIS) and scanning acoustic microscope (SAM), and to calculate their Pearson product moment correlations in the point of applying HFUIS for clinical use.

Methods: *Animals*: Six adult male Sprague-Dawley rats (16 weeks) were used in this study. The capsule of the knee was cut with a surgical knife and the joint was opened after administration of an overdose of sodium pentobarbital. After the ligaments and meniscus were resected, a cartilage-bone complex (3.8 mm in diameter) was obtained from the medial midcondylar region of the tibia with a cylindrical bar.

HFUIS: An electric impulse is generated by a high speed switching semiconductor. The electric pulse is used to excite a PVDF transducer with a central frequency of 120 MHz and a focal length of 3.2 mm.

HFUIS has three measurement modes (1.conventional C-mode acoustic microscope imaging of excised, thinly sliced tissue, 2. ultrasound impedance imaging of the surface of the tissue and 3. 3D ultrasound imaging visualizing the inside of tissue). A 3-D high frequency ultrasound microscope can make conventional C and B-mode images and make 3-D images reconstructed from B-mode images. Intensity was normalized by the reflection from a steel plate at the same distance.

SAM: The reflections from the tissue surface and from the interface between the tissue and the glass are received by the same transducer. The central frequency is 80 MHz. Frequency domain analysis of the reflection enables the separation of these two components and the calculation of the sound speed, tissue thickness and intensity by Fourier-transforming the waveform.

Tissue preparation: The specimens were immediately immersed in saline at room temperature before scanning with HFUIS. After the scanning, the specimens were immersed in 4% PFA in 0.1 M PBS. The fixed specimens were then decalcified and embedded in paraffin. The tissue was cut into 5-μm sagittal sections from the medial to the lateral side of the joint. After deparaffinization, the sections were assessed by SAM. The hematoxylin and eosin-stained sections were used to ensure morphological congruence in the analysis.

Image analysis: Relative intensity by HFUIS and the sound speed of the articular cartilage by SAM are calculated with gray scale images using commercially available image analysis software (PhotoShop CS2, Adobe Systems Inc., San Jose, CA). The articular cartilage is divided into three layers (superficial, middle and deep layers) and analyzed independently. We divided the articular cartilage, from the surface to the margin of the high intensity areas (subchondral bone) in HFUIS and high sound speed areas (subchondral bone) in SAM, into five areas. We defined the one-fifth from the surface as superficial layers and the rest as middle layers, and the average intensity by HFUIS and the sound speed by SAM were analyzed and their Pearson product moment correlations were calculated independently.

Results: The superficial and deep layers indicated high relative intensity, while the middle layer was inhomogeneous relative intensity by HFUIS. A high relative intensity by HFUIS and high sound speed area by SAM had strong correlations (Pearson product moment correlation, superficial layer: 0.704, middle layer: 0.731, deep layer: 0.258).

Conclusions: HFUIS made high resolution images of the articular cartilage and its intensity was strongly correlated with sound speed by SAM.

397

HIP BONE MINERAL DENSITY DOES NOT INFLUENCE TIBIOFEMORAL BONE MARROW LESION SIZE

J.B. Driban[1], G.H. Lo[2], L.L. Price[1], T.E. McAlindon[1]. *[1]Tufts Med. Ctr., Boston, MA, USA; [2]Baylor Coll. of Med., Houston, TX, USA*

Purpose: High hip bone mineral density (BMD) has been recognized as a potential risk factor for incident knee osteoarthritis (OA) but the relation between hip BMD and knee OA progression remains unclear. If hip BMD influences OA progression then the greatest influence may be on a bone-related OA lesion. Subchondral bone marrow lesions (BMLs), common OA-related magnetic resonance imaging (MRI) findings, can get larger and smaller over time and are associated with OA progression. No study has evaluated the relationship between hip BMD and knee BML size. Therefore, the purpose of this study was to evaluate the cross-sectional and longitudinal associations between hip (total hip and femoral neck) BMD and knee BML size.

Methods: The sample comprised 103 OA knees (Kellgren-Lawrence Grade [KLG] greater than or equal to 2) from participants in a randomized-clinical trial of vitamin D who had sagittal and coronal intermediate-weighted fat-suppressed (IW FS) 1.5-tesla MRIs and dual-energy x-ray absorptiometry (DXA) scans at baseline and 2-years. The IW FS sequences had a time to recovery (TR) of 2950 ms, time to echo (TE) of 31 ms, slice thickness of 3 mm, space thickness of 0.5 mm, and field of view (FOV) of 140 mm. We defined BMLs as regions of high-signal intensity on IW FS images located within 1.0 cm of hyaline cartilage and present on 2 or more sagittal or coronal images and classified them within 4 regions: index femur, index tibia, nonindex femur, and nonindex tibia. Two rheumatologists defined the index compartment as the compartment (medial or lateral) with greater pathology based on radiograph and MRI findings. We measured the maximal anterior-posterior, medial-lateral, and vertical dimensions of each BML. Their product represented the